Enhanced Transport during Pellet Injection in the Rijnhuizen Tokamak RTP

D. F. da Cruz, C. C. Chu, G. M. D. Hogeweij, N. J. Lopes Cardozo, A. A. M. Oomens, and F. J. Pijper
FOM-Instituut voor Plasmafysica "Rijnhuizen," Association Euratom-FOM, P.O. Box 1207, 3430 BE Nieuwegein, The Netherlands
(Received 15 March 1995)

The evolution of the radial profiles of electron temperature and density in a tokamak plasma during ablation of an injected hydrogen pellet is studied by Thomson scattering with a resolution of 1% of the mirror plasma radius. The energy content is hardly affected until the pellet reaches the sawtooth inversion radius when strongly enhanced transport sets in throughout the plasma. Asymmetric profiles are observed. Peaks of high density are formed, one of which often develops into a density "snake."

PACS numbers: 52.55.Fa, 28.52.Cx, 52.30.–q, 52.35.Ra

Injection of pellets of frozen H_2 or D_2 into the hot plasma is often considered the only serious candidate for efficient fueling of a thermonuclear fusion reactor. The ablation of the pellet, i.e., the evaporation, dissociation, and ionization, happens within a very short time interval ($\approx$300 μs in RTP). In this period the plasma density increases strongly while the temperature plummets. These dramatic changes may affect the stability of the plasma, the rates of thermal and particle transport, etc. A good understanding of the process of ablation and the complex interactions with the plasma is important in order to extrapolate to future devices. The perturbations of the plasma state induced by the pellet can also be used to probe fundamental processes in the plasma.

If the electron temperature (T_e) decreases in proportion with the increase of the electron density (n_e), the ablation process is referred to as adiabatic. In most existent models the ablation is assumed to be both adiabatic and local; i.e., the region not traversed by the pellet remains unperturbed. This assumption is justified only if radial transport of energy and particles is negligible during the ablation.

The question whether the ablation is adiabatic or not was probably first raised in a transport study in ASDEX [1], albeit without a clear answer. Measurements of the radial profile of the electron pressure (p_e) before and 2.5 ms after pellet ablation in JET [2] did support the adiabaticity. However, measurements in other machines [3,4] show that the assumption of adiabaticity is sometimes violated due to a rapid relaxation of the T_e profile. This process is known as precooling: The cooling front due to the pellet propagates faster than the pellet itself. These measurements were performed with limited spatial resolution ($\approx$10% in radius). In order to validate one of the models explaining the precooling [4,5], further measurements are required with higher spatial and temporal resolution.

We present n_e, T_e, and p_e profiles with a spatial resolution of 1% of the plasma radius, measured during pellet ablation with Thomson scattering (TS) in the RTP tokamak. The time of the measurements during the ablation process is scanned in a series of repeated plasma discharges. These measurements show that when the pellet reaches the sawtooth inversion radius, r_{inv}, fast transport sets in a rearrangement of the plasma electron energy is triggered. It is hypothesized that the pellet creates a large magnetic island, which leads to a breakdown of the thermal barrier at r_{inv} and to strongly enhanced transport throughout the plasma.

The measurements are done in discharges in RTP under the following conditions: major/minor radius $R_0 = 0.72$ m, $a = 0.164$ m, plasma current 80 kA, toroidal field 1.5 T, $n_e = (3\text{–}7) \times 10^{19}$ m^{-3}, $T_e = 0.6$ keV (central values), edge safety factor $q_a = 3.6$, and boronized vessel. Sawtooth activity is observed in most of these discharges, with $r_{\mathrm{inv}} = 30\text{–}40$ mm, measured with soft-x-ray tomography. A pellet is injected radially with a velocity of $v_{\mathrm{pel}} = 600$ m/s in the quasistationary phase of the discharge. A pellet contains $\approx 5 \times 10^{18}$ particles, which is about half of the total particle content of the target plasma. The velocity and the time of arrival of the pellet in the plasma are determined with two light detectors.

The key measurements in this study are performed with a Thomson scattering setup [6], which yields n_e, T_e, and p_e at 100 points along a vertical chord through the plasma center, with a resolution of 1.7 mm. Light from a pulsed 25 J ruby laser ($\lambda_0 = 693.3$ nm, beam 2 mm inner diam, pulse duration FWHM = 15 ns) is passed vertically through the plasma. The scattered light (scattering angle $\approx$90°) is imaged on a Littrow polychromator and detected with an ion-current-charged detector. At each z position, the spectrum is resolved into 85 channels, covering 550–850 nm. The toroidal angle between this instrument and the pellet injector is 60°.

During pellet ablation the intensities of the H_α and H_β lines are measured, viewing the ablation cloud along the pellet trajectory. Figure 1 shows a typical signal as a function of the pellet position (a constant v_{pel} is assumed). These measurements are very similar to observations in other tokamaks, therefore we assume that the ablation in RTP is typical for tokamaks.

By firing the laser of the TS diagnostic during the ablation ($\approx$250 μs) n_e, T_e, and p_e profiles are obtained.

 © 1995 The American Physical Society

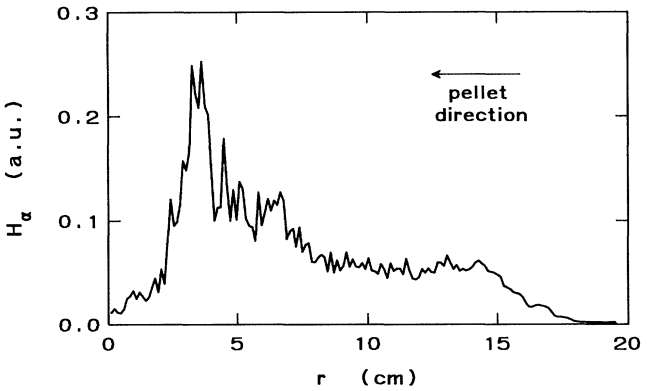

FIG. 1. Typical H_α signal measured during pellet ablation as a function of the radial position.

To measure the evolution of the profiles, a series of repeated discharges is used (only one laser shot can be given per discharge). The position of the pellet, r_{pel}, at the instant of the laser shot is determined assuming a constant v_{pel}. The uncertainty in v_{pel} results in an error in r_{pel} of ± 5 mm. Reference profiles are measured in similar discharges just before the pellet injection.

Four scans of r_{pel} were done with a total of 55 discharges. Typical examples of T_e, n_e, and p_e profiles obtained in one scan are presented in Fig. 2 for three values of r_{pel}. The virtual position of the pellet in the vertical direction, z_{pel}, is indicated in these pictures. The value of z_{pel} is calculated from r_{pel} (measured in the horizontal plane), assuming circular magnetic flux surfaces and a parabolic Shafranov shift profile. The examples in Fig. 2 represent three distinct phases during the ablation process: (a) $r_{\mathrm{pel}} > r_{\mathrm{inv}}$, (b) $0 < r_{\mathrm{pel}} < r_{\mathrm{inv}}$, and (c) the ablation is just finished. The profiles during ablation (closed symbols) are compared to reference profiles (open symbols). A reference pulse is selected of which the line averaged density ($\bar{n}_e$) agrees within

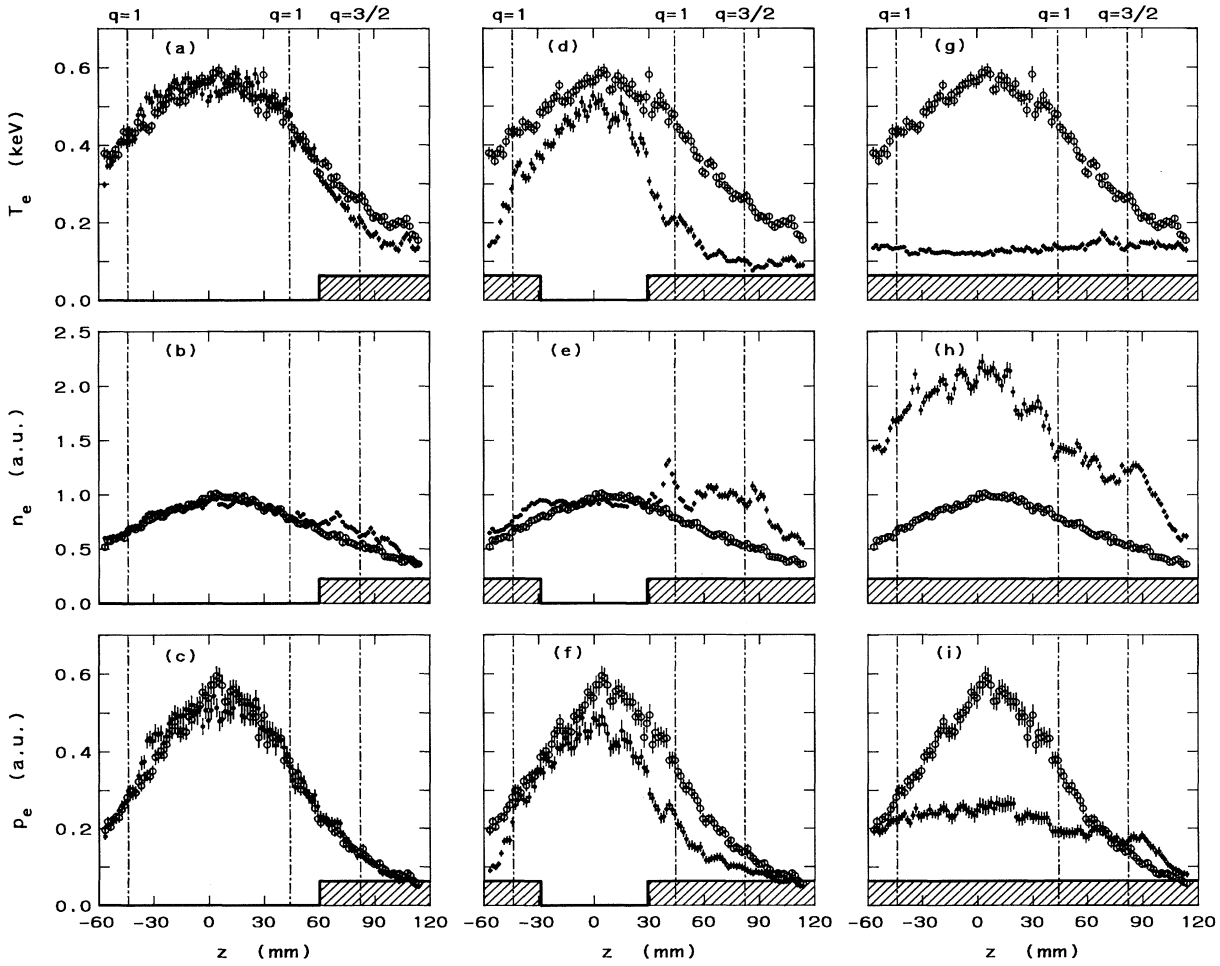

FIG. 2. Profiles of T_e, n_e, and p_e (•) measured with the TS diagnostic at the instant when the pellet is at $z_{\mathrm{pel}} = 60$ mm (a)–(c), $z_{\mathrm{pel}} = 29$ mm (d)–(f), and $z_{\mathrm{pel}} = -8.5$ mm (g)–(i), where negative values denote positions after the pellet crossed the plasma center. The horizontal bands indicate plasma positions already traversed by the pellet. The open symbols represent profiles before pellet injection.

20% with the prepellet $\bar{n}_e$ of the pulses shown in Fig. 2. To facilitate the comparison, the n_e profiles are scaled to make $\bar{n}_e$ before pellet injection identical. The same scaling factor is applied to the reference p_e profile. Also indicated in the plots are the positions of some rational flux surfaces, assuming a parabolic safety factor profile, $q(r)$ with $q(r_{\mathrm{inv}}) = 1$.

For $z_{\mathrm{pel}} = 60$ mm, a decrease of T_e is seen [Fig. 2(a)] for $z > z_{\mathrm{pel}}$, while peaks appear on the n_e profile [Fig. 2(b)]. The p_e profile [Fig. 2(c)] is virtually unchanged. This suggests a nearly adiabatic process. The symmetry of the profiles cannot be verified for $z_{\mathrm{pel}} > 60$ mm because of the limited z range of the TS diagnostic.

When the pellet penetrates to $z_{\mathrm{pel}} \leq 50$ mm a dramatic effect occurs in the plasma center [Figs. 2(d)–2(f)]. The p_e profile [Fig. 2(f)] collapses inside r_{inv}, even at positions not yet reached by the pellet. Clearly, the process does not remain adiabatic. Strong asymmetries of both the n_e and T_e are observed. The behavior of n_e in the plasma center is variable from shot to shot. There is no clear correlation between this diversity and variations either in the H_α signal or in the magnetohydrodynamic activity before the pellet injection.

When the ablation finishes [Figs. 2(g)–2(i)] obtained ≈ 150 μs after the pellet reached the plasma center], the T_e profile is flat with a value of $T_e \approx 120$ eV, while the n_e profile is peaked and still shows some local peaks. The p_e profile shows a further decrease in the plasma center, and some increase outside z_{inv}.

The electron energy content within a surface with radius r, $W_e(r)$, is calculated by integrating the p_e profile measured with the TS diagnostic from $z = -r$ to $z = r$, assuming toroidal symmetry. Clearly, this assumption is not justified with the strongly asymmetric profiles. However, in this way a zero order estimate of $W_e(r)$ can be obtained. The variation of this quantity relative to the prepellet value, $\Delta W_e(r)$, is shown in Fig. 3 as a function of z_{pel} for two values of r, i.e., $r = r_{\mathrm{inv}}$ and $r = 12$ cm (the extent of the TS measurements). The plots suggest that the ablation remains nearly adiabatic until the pellet reaches r_{inv}. At that moment, a fast redistribution of kinetic energy takes place and 25% of $W_e(r)$ is lost in $t_{\mathrm{loss}} \approx 50$ μs. This loss cannot be ascribed to energy exchange between electrons and ions, since in the worst case its contribution is not more than 5%. In reality, it will be smaller or it could be even negative. The decrease of the central energy content, $\Delta W_e(r_{\mathrm{inv}})$, accounts for 60% of the total decrease in energy content, $\Delta W_e(r = 12$ cm). We calculated the electron heat flux $q_e(r)$ needed to provoke the observed decrease of $W_e(r)$ during the ablation. Other elements in the power balance were neglected in this calculation, since their effect on $q_e(r)$ is more than an order of magnitude smaller. Assuming that the energy loss process is diffusive, and effective $\chi_e(r)$ has been calculated from $q_e(r)$ and grad$[T_e(r)]$. Until the pellet reaches r_{inv}, $\chi_e(r)$

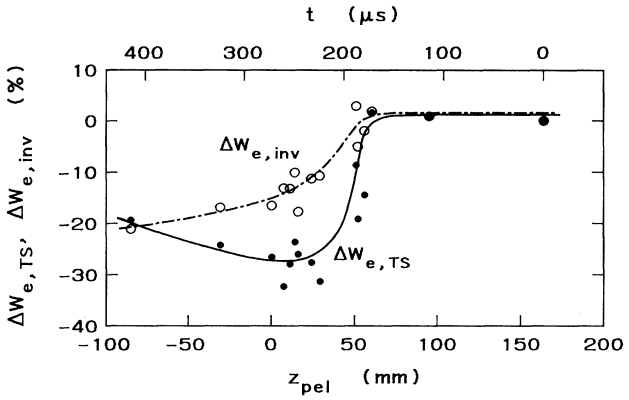

FIG. 3. The dependence on the pellet position of the variation of the electron energy in the plasma region observed with the TS diagnostic ($\Delta W_{e,\mathrm{TS}}$) and inside the sawtooth inversion radius ($\Delta W_{e,\mathrm{inv}}$) relative to the prepellet value.

is only slightly enhanced. During the pellet penetration from r_{inv} to the center of the plasma $\chi_e(r)$ attains very high values throughout the plasma: ~ 20 m^2/s near r_{inv} and ~ 100 m^2/s in the outer part of the plasma. This corresponds to a temporary increase of χ_e by 2 orders of magnitude over the prepellet value. This high diffusivity is only present during the 50 μs of rapid loss, and is attributed to stochastization of the field. The slower decay of $\Delta W_e(r_{\mathrm{inv}})$ can be explained by the radial variation of χ_e. Note that in the rapid loss phase the transport is probably not diffusive, so that χ_e is not more than a rough measure of the transport. Similar observations have been made on TFR during pellet ablation [7], for which the electron cyclotron emission signals measuring inside the $q = 1$ surface decay more slowly than those outside.

Finally, after the ablation process is over, in most RTP discharges in which the pellet penetrates to r_{inv} a $m = n = 1$ density perturbation, a so-called "snake" (first seen in JET [8]), is observed with soft-x-ray tomography. The snake persists for tens of milliseconds, which is much longer than the global energy or particle confinement time in RTP.

These detailed profile measurements demonstrate that as long as the pellet has not reached r_{inv}, the ablation process is indeed nearly adiabatic. In some cases a small loss of pressure is observed in this phase, but this is a minor effect.

A second aspect is given by the density peaks that appear in the wake of the pellet. There are two possible explanations for this phenomenon: either the peaks are magnetic islands or they are caused by ablatant streaming along field lines with finite velocity. Figure 4 shows the trajectory of the pellet mapped onto the poloidal plane of the TS diagnostic, assuming parabolic q profile as before and a rigid toroidal plasma rotation of 12 kHz. It is clear from this figure that, purely because of the finite transport rate of the ablatant, peaks in the measured n_e profile must

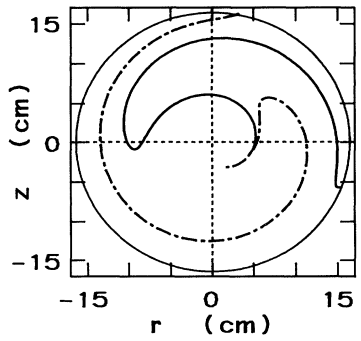

FIG. 4. Trajectory of the pellet as seen in the poloidal plane of the TS diagnostic after one toroidal turn, for both parallel to the plasma current (dashed line) and antiparallel (solid line) expansion of the ablatant along field lines.

be expected. The effect on p_e is expected to be much less pronounced, in agreement with the observations. An exception is the peak near r_{inv}, which is discussed below.

Even if the density peaks need not be magnetic islands, the measurements demonstrate that the localized source does induce strong asymmetries of n_e and T_e. These will lead to the development of islands, which can play a role in the nonadiabatic phase discussed below.

A third important result of the present measurements is that they show that the rapid loss of energy is triggered sharply (within ≈ 10 μs) when the pellet crosses r_{inv}. To explain the loss of energy in the ensuing 40 μs, a global enhancement of the transport must be invoked. A detailed analysis of many profiles measured in this phase will be undertaken to get more insight into the loss process.

The profile measurements corroborate and complement results obtained from the TEXTOR tokamak [9]. In that experiment, pellet injection led to a fast loss of runaway electrons, while also some global loss of pressure occurred. The losses were attributed to ergodization of the field due to the overlap of large magnetic islands, in particular, $m = n = 1$ and $m/n = 2/1$. During the short period of strong ergodization a large remnant $m = n = 1$ island remained intact, as was demonstrated by a persistent beam of runaway electrons with an $m = n = 1$ structure.

The same picture appears to describe the events in RTP. The measurements show that the ergodicity develops within ≈ 10 μs when the pellet crosses r_{inv}. It is hypothesized that at that moment the $m = n = 1$ mode is driven strongly unstable, producing a large magnetic island. This island could develop into the snake observed later. The interaction of the $m = n = 1$ island with the higher m islands produced in the wake of the pellet would lead to stochastization of the field, and thus to a rapid energy loss. Since the loss period has a duration of only ≈ 40 μs, it appears that the field topology is also quickly restored. This could be the result of the fast transport itself, which reduces the gradients and asymmetries of the profiles.

It is important to note that the effective diffusivity has to assume temporarily a value that exceeds the normal value by orders of magnitude. In [7] the possible presence of a thermal barrier has been proposed. Further evidence for such a toroidal shell of low diffusivity near r_{inv} is given in [10]. To allow the rapid loss, this insulating shell must be broken. However, this is not sufficient: The effective diffusivity must be enhanced throughout the plasma. These requirements are well met by the picture of large overlapping islands creating an ergodic field: The thermal barrier is thought to be related to a region of "good" flux surfaces just outside the $q = 1$ surface, where the density of low order rational q surfaces is minimal. Such a good surface is broken if an overlap of islands occurs.

The authors wish to acknowledge the careful reading of the manuscript and helpful conversations with F. C. Schüller, A. Montvai, and B. C. Schokker. We also thank the RTP team for the operation of the tokamak and diagnostics. This work was performed under the Euratom-FOM association agreement, with financial support from NWO and Euratom.

[1] G. Vlases *et al.*, in *Proceedings of the 11th European Conference on Controlled Fusion and Plasma Physics, Aachen, 1983* (European Physical Society, Geneva, 1983), Vol. 1, p. 127.
[2] L. R. Baylor *et al.*, Nucl. Fusion **32**, 2177 (1992).
[3] M. Sakamoto *et al.*, Plasma Phys. Controlled Fusion **33**, 583 (1991).
[4] W. Liu and M. Talvard, Nucl. Fusion **34**, 337 (1994).
[5] J. O'Rourke, Nucl. Fusion **27**, 2075 (1987).
[6] C. C. Chu *et al.*, in *Proceedings of the 21st European Conference on Controlled Fusion and Plasma Physics, Montpellier, 1994* (European Physical Society, Geneva, 1994), Vol. 18B, Pt. III.
[7] TFR Group, Nucl. Fusion **27**, 1975 (1987).
[8] A. Weller *et al.*, Phys. Rev. Lett. **59**, 2303 (1987).
[9] R. Jaspers *et al.*, Phys. Rev. Lett. **72**, 4093 (1994).
[10] N. J. Lopes Cardozo *et al.*, Phys. Rev. Lett. **73**, 256 (1994).